Theoretical Examination of Mg 2+ −Mediated Hydrolysis of a Phosphodiester Linkage as Proposed for the Hammerhead Ribozyme

ARTICLE *in* JOURNAL OF THE AMERICAN CHEMICAL SOCIETY · SEPTEMBER 2003

Impact Factor: 12.11 · DOI: 10.1021/ja021451h · Source: PubMed

5 AUTHORS, INCLUDING:

Rhonda A Torres

18 PUBLICATIONS **612** CITATIONS

SEE PROFILE

Louis Noodleman

The Scripps Research Institute

136 PUBLICATIONS **9,336** CITATIONS

SEE PROFILE

J|A|C|S
ARTICLES
Published on Web 07/17/2003

Theoretical Examination of Mg^{2+}-Mediated Hydrolysis of a Phosphodiester Linkage as Proposed for the Hammerhead Ribozyme

Rhonda A. Torres,*,† Fahmi Himo,†,§ Thomas C. Bruice,‡ Louis Noodleman,† and Timothy Lovell*,†

Contribution from the Department of Molecular Biology TPC-15, The Scripps Research Institute, La Jolla, California 92037, and Department of Chemistry and Biochemistry, University of California, Santa Barbara, California 93106

Received December 16, 2002; Revised Manuscript Received April 2, 2003; E-mail: torres@scripps.edu; tlovell@scripps.edu

Abstract: The hammerhead ribozyme is an RNA molecule capable of self-cleavage at a unique site within its sequence. Hydrolysis of this phosphodiester linkage has been proposed to occur via an in-line attack geometry for nucleophilic displacement by the 2′-hydroxyl on the adjoining phosphorus to generate a 2′,3′-cyclic phosphate ester with elimination of the 5′-hydroxyl group, requiring a divalent metal ion under physiological conditions. The proposed $S_N2(P)$ reaction mechanism was investigated using density functional theory calculations incorporating the hybrid functional B3LYP to study this metal ion-dependent reaction with a tetraaquo magnesium (II)-bound hydroxide ion. For the Mg^{2+}-catalyzed reaction, the gas-phase geometry optimized calculations predict two transition states with a kinetically insignificant, yet clearly defined, pentacoordinate intermediate. The first transition state located for the reaction is characterized by internal nucleophilic attack coupled to proton transfer. The second transition state, the rate-determining step, involves breaking of the exocyclic P−O bond where a metal-ligated water molecule assists in the departure of the leaving group. These calculations demonstrate that the reaction mechanism incorporating a single metal ion, serving as a Lewis acid, functions as a general base and can afford the necessary stabilization to the leaving group by orienting a water molecule for catalysis.

1. Introduction

The hammerhead ribozyme is a small, self-catalytic RNA molecule that makes up the genome of several plant viruses and virusoids[1,2] and is composed of a single-stranded region of 15 nucleotides, flanked by three Watson−Crick base-paired stems.[3,4] In this central consensus region,[5] the cleavage of the phosphodiester backbone occurs at a discrete location; and, as with some protein enzymes that catalyze biochemical reactions or transformations in nucleic acids, requires divalent metal ions as cofactors to promote activity at physiological conditions.[6] In the absence of divalent metal ions, the half-life of the hydroxide-catalyzed solvolysis of the RNA backbone as been estimated to be approximately 110 years at pH7 and 25 °C;[7] however, in their presence, these rates are reduced to the order of seconds to minutes.[3,8] The metal ion typically utilized by the organisms to activate the phosphate moiety in the phosphodiester linkage for catalysis of hydrolysis in this ribozyme is Mg^{2+}, although other metal ions have been shown to promote catalysis in vitro.[9−12]

The mechanism of nucleophilic displacement at the phosphorus has been proposed to be $S_N2(P)$ with an in-line geometry, where the approach of the $2'O^-$ to the phosphorus is at a 180° angle relative to the leaving 5′-oxygen[13] with inversion of configuration about the phosphorus (Scheme 1).[14−19] The other plausible mechanism for nucleophilic displacement at the phosphorus, the adjacent attack geometry, is unlikely as the steric requirement associated with pseudorotation of the leaving group prior to its departure is made quite difficult due to the structure of the RNA molecule.[13] The log of the cleavage rate between pH 5.7 and 8.9 was shown to increase linearly with a

† The Scripps Research Institute.
‡ University of California.
§ Present Address: Royal Institute of Technology, SCFAB, Department of Biotechnology, Theoretical Chemistry, S-106 91 Stockholm, Sweden.

(1) Forster, A. C.; Symons, R. H. *Cell* **1987**, *50*, 9−16.
(2) Forster, A. C.; Symons, R. H. *Cell* **1987**, *49*, 211−220.
(3) Uhlenbeck, O. C. *Nature* **1987**, *328*, 596−600.
(4) Ruffner, D. E.; Stormo, G. D.; Uhlenbeck, O. C. *Biochemistry* **1990**, *29*, 10695−10702.
(5) Buzayan, J. M.; Gerlach, W. L.; Bruening, G. *Proc. Natl. Acad. Sci. U.S.A.* **1986**, *83*, 8859−8862.
(6) Blaskó, A.; Bruice, T. C. *Acc. Chem. Res.* **1999**, *32*, 475−484.
(7) Williams, N. H.; Takasaki, B.; Wall, M.; Chin, J. *Acc. Chem. Res.* **1999**, *32*, 485−493.
(8) Fedor, M. J.; Uhlenbeck, O. C. *Biochemistry* **1992**, *31*, 12042−12054.
(9) Kuimelis, R. G.; McLaughlin, L. W. *Nucleic Acids Res.* **1995**, *23*, 4753−4760.
(10) Kuimelis, R. G.; McLaughlin, L. W. *Biochemistry* **1996**, *35*, 5308−5317.
(11) Dahm, S. C.; Derrick, W. B.; Uhlenbeck, O. C. *Biochemistry* **1993**, *32*, 13040−13045.
(12) Dahm, S. C.; Uhlenbeck, O. C. *Biochemistry* **1991**, *30*, 9464−9469.
(13) Westheimer, F. H. *Acc. Chem. Res.* **1968**, *1*, 70−78.
(14) Slim, G.; Gait, M. J. *Nucleic Acids Res.* **1991**, *19*, 1183−1188.
(15) Koizumi, M.; Ohtsuka, E. *Biochemistry* **1991**, *30*, 5145−5150.
(16) van Tol, H.; Buzayan, J. M.; Feldstein, P. A.; Eckstein, F.; Bruening, G. *Nucleic Acids Res.***1990**, *18*, 1971−1975.
(17) Usher, D. A. *Proc. Natl. Acad. Sci. U.S.A.* **1969**, *62*, 661−667.
(18) Usher, D. A.; Erenrich, E. S.; Eckstein, F. *Proc. Natl. Acad. Sci. U.S.A.* **1972**, *69*, 115−118.
(19) Usher, D. A.; Richardson, D. I.; Eckstein, F. *Nature* **1970**, *228*, 663−665.

Scheme 1

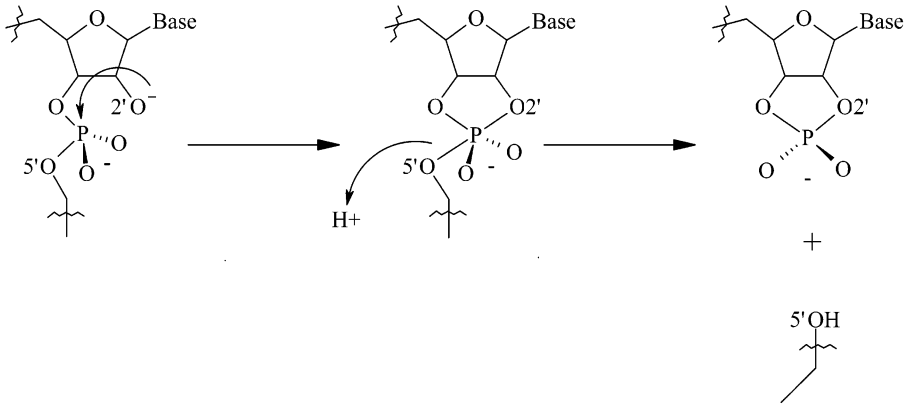

Scheme 2

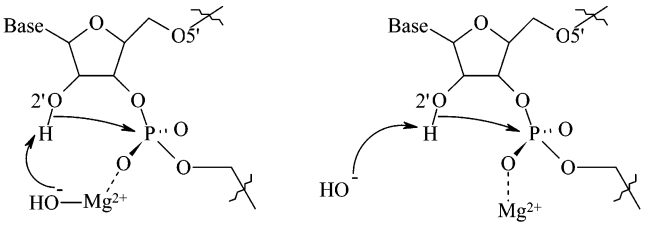

slope approximately equal to one,[11,20,21] suggesting a single deprotonation event is required for cleavage. It has also been shown experimentally that a metal ion ligates to the *pro-R*$_P$ oxygen of the $-O-(PO_2^-)-O-$ group undergoing reaction, a feature crucial in the metal ion catalysis of phosphodiesters as cancellation of the negative charge allows for nucleophilic addition to phosphorus (Scheme 2).[6,14,15,22−24] The metal ion can provide a ligated hydroxide to remove the proton from the 2′OH to generate the nucleophile (general base catalysis) or the nucleophile can be generated by a lyate HO^- (specific base catalysis) and the metal ion has an alternate role in the reaction. This divalent metal ion, or possibly another, can provide the necessary stabilization to the leaving group either by direct interaction with the leaving-group oxygen or by orienting a water molecule such that a proton can be donated to this group. The way in which stabilization of the leaving group is achieved is a subject of debate.[25−27] Thus, despite the numerous experiments performed on many different hammerhead ribozyme motifs, the precise details of the mechanism of hydrolysis and the number of metal ions essential in the cleavage reaction of the hammerhead ribozyme are not known.

Crystal structures of the hammerhead ribozyme as inhibitor, substrate, or modified substrate complexes have been solved.[28−31] These structures have provided invaluable information regarding the structure of the hammerhead ribozyme as well as additional insight into the metal ion binding sites of this molecule. Of these metal ion binding sites, at least one appears necessary to achieve proper folding and to stabilize or position other essential functional groups, while one or more additional divalent metal ions participate in the cleavage reaction.[12] None of these crystal structures, however, show the 2′-hydroxyl group poised for an in-line displacement of the 5′-leaving group. In an effort to discover the structural rearrangements that would lead to conformations consistent with an in-line displacement, these crystal structures have formed the basis of molecular dynamics (MD) simulations on this system.[32−37] Of these MD studies, only one[37] showed the spontaneous rearrangement of the hammerhead ribozyme from the published crystal structure to give near in-line attack conformations (NACs,[38,39] Figure 1) and revealed the potential roles of the conserved core residues. We refer the reader to ref 37 for additional details.

Several groups have performed quantum mechanical studies on the hydrolysis of phosphodiesters in an effort to provide a detailed description of the mechanism in the hammerhead ribozyme.[40−43] A transition state has been located which depicts the P−O bond cleavage as the rate-determining step along the reaction coordinate; however, it was characterized by rotations of P−O bonds, an event that is highly improbable in the hammerhead ribozyme system. In addition, none of these investigations into the base-catalyzed reaction incorporated a tetraaquo Mg(II) ion which completes the first coordination sphere and is likely the state of the metal ion in solution.

(20) O'Rear, J. L.; Wang, S.; Feig, A. L.; Beigelman, L.; Uhlenbeck, O. C.; Herschlag, D. *RNA* **2001**, *7*, 537−545.
(21) Curtis, E. A.; Bartel, D. P. *RNA* **2001**, *7*, 546−552.
(22) Bruice, T. C.; Tsubouchi, A.; Dempcy, R. O.; Olson, L. P. *J. Am. Chem. Soc.* **1996**, *118*, 9867−9875.
(23) Vanhommerig, S. A. M.; Sluyterman, L. A. ×ae.; Meijer, E. M. *Biochim. Biophys. Acta−Protein Struct. Mol. Enzymol.* **1996**, *1295*, 125−138.
(24) Dempcy, R. O.; Bruice, T. C. *J. Am. Chem. Soc.* **1994**, *116*, 4511−4512.
(25) Cowan, J. A. *Chem. Rev.* **1998**, *98*, 1067−1087.
(26) Kuimelis, R. G.; McLaughlin, L. W. *Chem. Rev.* **1998**, *98*, 1027−1044.
(27) Zhou, D. M.; Taira, K. *Chem. Rev.* **1998**, *98*, 991−1026.
(28) Murray, J. B.; Dunham, C. M.; Scott, W. G. *J. Mol. Bio.* **2002**, *315*, 121−130.
(29) Murray, J. B.; Terwey, D. P.; Maloney, L.; Kerpelsky, A.; Usman, N.; Beigelman, L.; Scott, W. G. *Cell* **1998**, *92*, 665−673.
(30) Scott, W. G.; Finch, J. T.; Klug, A. *Cell* **1995**, *81*, 991−1002.
(31) Scott, W. G.; Murray, J. B.; Arnold, J. R. P.; Stoddard, B. L.; Klug, A. *Science* **1996**, *274*, 2065−2069.
(32) Mei, H. Y.; Kaaret, T. W.; Bruice, T. C. *Proc. Natl. Acad. Sci. U.S.A.* **1989**, *86*, 9727−9731.
(33) Setlik, R. F.; Shibata, M.; Sarma, R. H.; Sarma, M. H.; Kazim, A. L.; Ornstein, R. L.; Tomasi, T. B.; Rein, R. *J. Biomol. Struct. Dyn.* **1995**, *13*, 515−522.
(34) Hermann, T.; Auffinger, P.; Westhof, E. *Eur. Biophys. J.* **1998**, *27*, 153−165.
(35) Hermann, T.; Auffinger, P.; Scott, W. G.; Westhof, E. *Nucleic Acids Res.* **1997**, *25*, 3421−3427.
(36) Torres, R. A.; Bruice, T. C. *Proc. Natl. Acad. Sci. U.S.A.* **1998**, *95*, 11077−11082.
(37) Torres, R. A.; Bruice, T. C. *J. Am. Chem. Soc.* **2000**, *122*, 781−791.
(38) Lightstone, F. C.; Bruice, T. C. *J. Am. Chem. Soc.* **1994**, *116*, 10789−10790.
(39) Lightstone, F. C.; Bruice, T. C. *J. Am. Chem. Soc.* **1996**, *118*, 2595−2605.
(40) Storer, J. W.; Uchimaru, T.; Tanabe, K.; Uebayasi, M.; Nishikawa, S.; Taira, K. *J. Am. Chem. Soc.* **1991**, *113*, 5216−5219.
(41) Uebayasi, M.; Uchimaru, T.; Koguma, T.; Sawata, S.; Shimayama, T.; Taira, K. *J. Org. Chem.* **1994**, *59*, 7414−7420.
(42) Uchimaru, T.; Tanabe, K.; Nishikawa, S.; Taira, K. *J. Am. Chem. Soc.* **1991**, *113*, 4351−4353.
(43) Lim, C.; Karplus, M. *J. Am. Chem. Soc.* **1990**, *112*, 5872−5873.

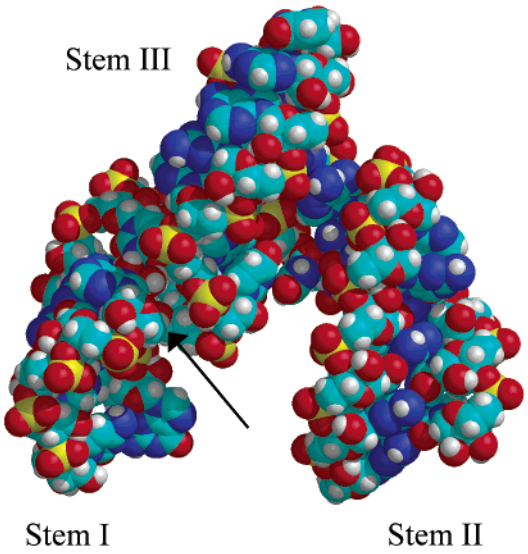

Figure 1. Global conformation of a hammerhead ribozyme obtained during molecular dynamics simulations[37] in a near in-line attack Conformation (NAC) displaying a relative orientation of the Watson−Crick base-paired stems as found in the X-ray crystal structure solved by Scott and co-workers.[31] The starting geometry of **I** for the geometry optimizations performed in this study was taken from the coordinates of the ribose ring of Residue C17 and the adjacent phosphate (A1.1). The arrow indicates the site where cleavage takes place.

Scheme 3

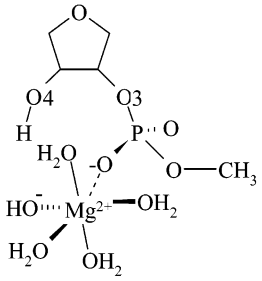

I

Incorporation of explicit water molecules has resulted in an improved representation of the computational model in theoretical investigations of acid-catalyzed phosphodiester hydrolysis.[44] Using Car−Parinello combined DFT-molecular dynamics calculations, Boero et al. examined reaction mechanisms for a model phosphodiester in a system, which also contained 62 water molecules. For this ribose phosphodiester in water, as a 1^- anion, the authors found a very high reaction barrier (∼57 kcal/mol) when the system was driven through the P−O2′ bond-formation reaction coordinate. When Mg^{2+} was incorporated in the system, as $Mg^{2+}(H_2O)_5$, in contrast to our model $Mg^{2+}(HO^-)\ (H_2O)_4$ shown in Scheme 3, Boero et al. find that the Mg^{2+} ion is ineffective in phosphodiester hydrolysis, although the activation energy for deprotonating the O2′ is lowered.

In our quantum mechanical investigation, we expand upon the results of our previous molecular dynamics studies and those of previous quantum mechanical studies on this system. We utilize the neutral chemical model, a mixed phosphodiester of methanol and 3,4-dihydroxytetrahydrofuran (charge = −1) with a $[Mg^{2+}(HO^-)\ (H_2O)_4]^{1+}$ bound to the *pro-*R_P oxygen (**I**, Scheme 3) using the B3LYP density functional theory (DFT) method to investigate the rate-determining step in the hammerhead ribozyme reaction, cleavage of the P−OCH_3 (P−OR) bond. This study focuses on the plausibility of a mechanism involving one metal ion catalysis of hydrolysis in the hammerhead ribozyme and includes an Mg^{2+} ion with a complete first-coordination sphere to represent the immediate environment of this divalent metal ion at the active site.

2. Methods

All geometries and subsequent energies calculated in this study were performed using the B3LYP density functional theory[45−47] method implemented in the Gaussian98 program package.[48] Geometry optimizations utilized the double-ζ plus polarization basis set 6-31G(d,p), followed by single-point energy calculations using the 6-311+G(2d,-2p) basis set. The calculations performed were spin restricted as expected for Mg^{2+}, as it is redox innocent and not a transition metal. Hessians were calculated at the B3LYP/6-31G(d,p) level of theory and allow for the evaluation of zero-point vibrational effects on the energy. The Hessians indicate that the located stationary points are correct, such that no imaginary frequencies exist for minima and one imaginary frequency exists for transition states. The effect of solvent was modeled with the conductor-like solvation model COSMO[49] at the B3LYP/6-31G(d,p) level. In this model, a cavity around the system of interest is surrounded by a polarizable continuum dielectric, here chosen to be the standard for aqueous solution $\epsilon = 80$, and a single-point calculation was performed on the gas-phase geometry. With the exception of the dielectric constant, default values were used in the COSMO calculations. A Mulliken population analysis was used for the charge densities. All energies discussed below include the zero-point energy (ZPE) correction, entropy, and solvation effects. Typical errors reported for B3LYP are about 2−3 kcal/mol for reaction barriers and energies for complexes without transition metals.[50−52] However, this performance is variable, depending on the type of system and reaction. Experimental and computational data for reaction barriers are both less reliable and less available, in general.

3. Results and Discussion

The effect of general base catalysis (Scheme 2) in the hammerhead ribozyme self-cleavage reaction was examined using a model compound, **I**, given in Scheme 3. The starting structure for this study was taken from a near in-line attack conformation (NAC)[38,39] obtained during molecular dynamics studies[37] performed using the 3.0 Å resolution crystal structure solved by Scott et al.[31] The Mg^{2+}-ligated hydroxide group was generated by removing a proton from a Mg^{2+}-bound water adjacent to the 2′-OH in the NAC structure (ref 37, Figure 4).

(44) Boero, M.; Terakura, K.; Tateno, M. *J. Am. Chem. Soc.* **2002**, *124*, 8949−8957.
(45) Becke, A. D. *J. Chem. Phys.* **1986**, *84*, 4524−4529.
(46) Becke, A. D. *Phys. Rev. A: At., Mol., Opt. Phys.* **1988**, *38*, 3098−3100.
(47) Lee, C.; Yang, W.; Parr, R. G. *Phys. Rev. B: Condens. Matter* **1988**, *37*, 785−789.
(48) Frisch, M. J.; Trucks, G. W.; Schlegel, H. B.; Scuseria, G. E.; Robb, M. A.; Cheeseman, J. R.; Zakrzewski, V. G.; Montgomery, J. A., Jr.; Stratmann, R. E.; Burant, J. C.; Dapprich, S.; Millam, J. M.; Daniels, A. D.; Kudin, K. N.; Strain, M. C.; Farkas, O.; Tomasi, J.; Barone, V.; Cossi, M.; Cammi, R.; Mennucci, B.; Pomelli, C.; Adamo, C.; Clifford, S.; Ochterski, J.; Petersson, G. A.; Ayala, P. Y.; Cui, Q.; Morokuma, K.; Malick, D. K.; Rabuck, A. D.; Raghavachari, K.; Foresman, J. B.; Cioslowski, J.; Ortiz, J. V.; Baboul, A. G.; Stefanov, B. B.; Liu, G.; Liashenko, A.; Piskorz, P.; Komaromi, I.; Gomperts, R.; Martin, R. L.; Fox, D. J.; Keith, T.; Al-Laham, M. A.; Peng, C. Y.; Nanayakkara, A.; Challacombe, M.; Gill, P. M. W.; Johnson, B.; Chen, W.; Wong, M. W.; Andres, J. L.; Gonzalez, C.; Head-Gordon, M.; Replogle, E. S.; Pople, J. A. *Gaussian 98*; Gaussian, Inc.: Pittsburgh, PA, 1998.
(49) Klamt, A.; Schuurman, G. *J. Chem. Soc., Perkins Trans. 2* **1993**, *5*, 799−805.
(50) Grimme, S. *J. Chem. Phys.* **2003**, *118*, 9095−9102.
(51) Koch, W.; Holthausen, M. C. *A Chemist's Guide to Density Functional Theory*, 2nd ed.; Wiley-VCH: Weinheim, 2001.
(52) Lynch, B. J.; Truhlar, D. G. *J. Phys. Chem. A* **2001**, *105*, 2936−2941.

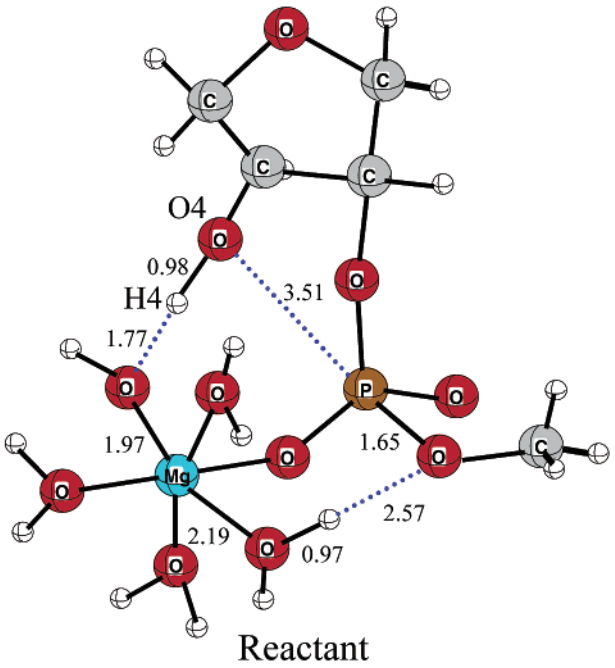

Figure 2. Optimized structure of the Reactant, **I**.

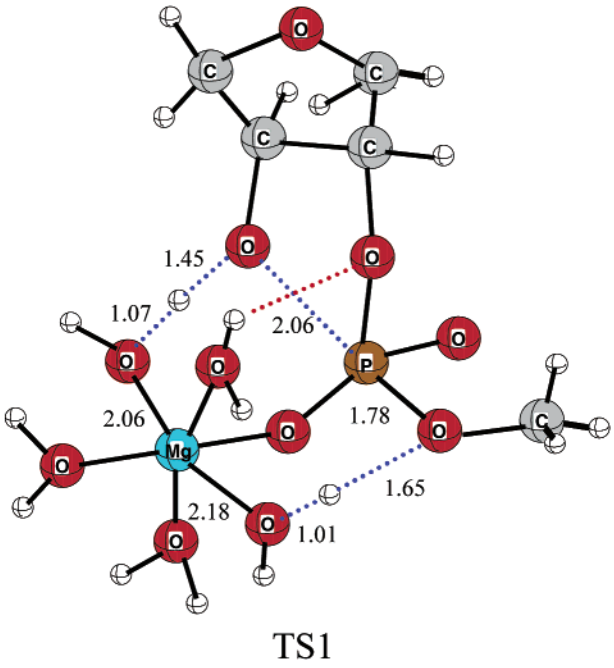

Figure 3. Optimized structure of the first transition state (TS1) located depicting proton-transfer coupled with nucleophilic attack on the scissile phosphate.

Table 1. Relevant Distances (in Å) and Angle (in degrees) for the Structures in the Catalysis of Hydrolysis for Compound **I**

species	O4–P	P–OCH_3	H4–$^-$OH	H_{wat}–OCH_3	O4–P–OCH_3
reactant	3.51	1.65	1.77	2.57	143.1
TS1	2.06	1.78	1.07	1.65	157.5
intermediate	1.98	1.80	1.05	1.61	157.4
TS2	1.84	1.96	1.00	1.28	157.8
product	1.69	5.57	0.98	1.00	100.4

Table 2. Summary of the Energies (in kcal/mol) in the Base-Catalyzed Nucleophilic Attack on Phosphorus in Compound **I**

species	ΔE	ΔE_{ZPE}	ΔE_{solv}	$\Delta E_{entropy}$	ΔE_{total}
reactant	0	0	0	0	0
TS1	29.8	−0.9	−9.7	−0.6	18.6
intermediate	30.1	−0.7	−10.3	−0.5	18.6
TS2	31.0	−1.9	−7.9	−0.4	20.8
product	−6.5	0.9	1.3	2.0	−2.3

The use of $Mg^{2+}(HO^-)$ reflects the proposal that a metal-bound hydroxide acts as the base in metal ion-catalyzed reactions of the hammerhead ribozyme.[11] This chemical model is charge neutral and incorporates an octahedrally coordinated Mg^{2+} (aq) ion.[25] This chemical model also incorporates the basic features and necessary functional groups to adequately model the proposed hydrolysis reaction for the hammerhead ribozyme.[44,53] A NAC for this system was defined previously as having an attack distance (oxygen−phosphorus) of ≤3.25 Å and attack angle of ≥150°.[36,37]

3.1. Reactant Species. Geometry optimizations on the starting structure obtained from molecular dynamics simulations provided the reactant species shown in Figure 2. Here, the O4 to P distance is 3.51 Å and the O4−P−OCH_3 angle is 143.1° (Table 1) with the five-membered furanose ring in the *S* puckering domain as seen in ribo- and deoxyribonucleosides.[54] MD simulations performed on crystal structures and model systems of the hammerhead ribozyme have suggested that it is necessary for the furanose ring to be in the *S* (C2′-*endo*) puckering domain for nucleophilic attack on the scissile phosphate to proceed.[32,34−37] The furan ring remains in the *S* puckering domain throughout the geometry optimizations (vide infra). This structure is no longer a NAC structure as previously defined for this system.[36,37] Here, a hydrogen bond occurs between the negatively charged oxygen atom of the $Mg^{2+}(HO^-)$ (aq) and the proton of the O4 moiety. The hydrogen to be transferred is still bound to the O4 of the substrate with an O−H distance of 0.98Å, and the P−OCH_3 distance associated with the eventual departure of the leaving group is 1.65Å. There is a very weak hydrogen-bonding interaction[55−58] between the trans water molecule, adjacent to the methoxy oxygen of the leaving group, with an oxygen−oxygen distance of 3.54 Å.

3.2. Generation of Nucleophile, Transition State 1. Performing a transition state search resulted in the location of the first transition state (TS1, Figure 3) in this reaction. Here, the ring of the transition-state structure (as well as for the intermediate and second transition-state structure, vide infra) spans one apical and one equatorial position in accord with the proposed mechanism for hydrolysis in cyclic phosphate esters.[59] This structure has one imaginary frequency at −137 cm^{-1} corresponding to the transfer of the proton from O4 to the Mg^{2+}-bound HO− group that is coupled with the nucleophilic attack of the $O4^-$ on the scissile phosphate. The energy of this structure, ΔE_{total}, is calculated to be +18.6 kcal/mol, relative to the Reactant (Table 2). In this asymmetric transition-state structure, the O4−P distance (attack distance) is 2.06 Å and the O4−P−OCH_3 angle (angle for nucleophilic displacement)

(53) Lyne, P. D.; Karplus, M. *J. Am. Chem. Soc.* **2000**, *122*, 166−167.
(54) Saenger, W. *Principles of Nucleic Acid Structure.*; Springer: New York, 1984.
(55) Cleland, W. W.; Kreevoy, M. M. *Science* **1994**, *264*, 1887−1890.
(56) Frey, P. A.; Whitt, S. A.; Tobin, J. B. *Science* **1994**, *264*, 1927−1930.
(57) Gerlt, J. A.; Gassman, P. G. *J. Am. Chem. Soc.* **1993**, *115*, 11552−11568.
(58) Gerlt, J. A.; Gassman, P. G. *Biochemistry* **1993**, *32*, 11943−11952.
(59) Haake, P. C.; Westheimer, F. H. *J. Am. Chem. Soc.* **1961**, *83*, 1102−1109.

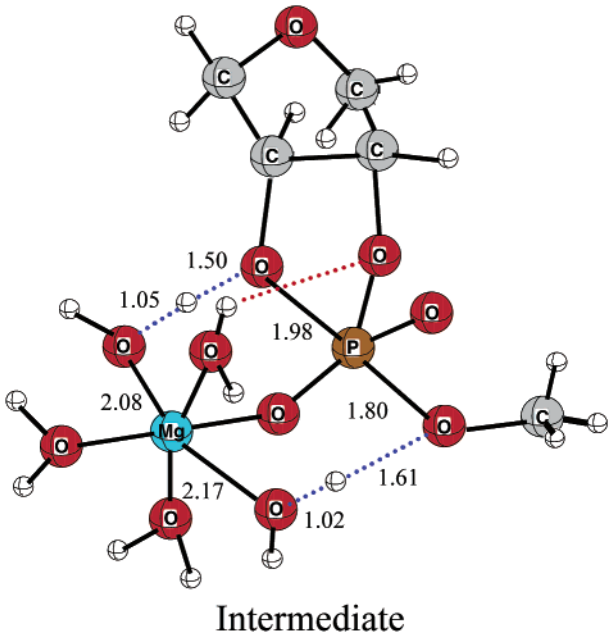

Figure 4. Optimized structure of the pentacoordinate phosphorane intermediate.

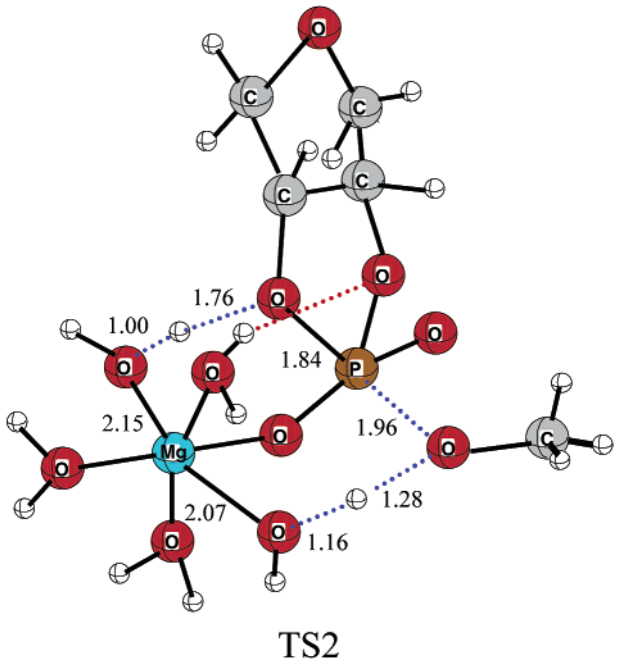

Figure 5. Optimized structure of the second transition state (TS2): the rate-determining step for phosphodiester hydrolysis.

is 157.5° (Table 1). It was found that the phosphorus and equatorial oxygen atoms are nearly planar (+5.8° phosphorus deviation above plane) in contrast to that observed in the Reactant (+24.0° deviation). The proton (H4) on O4 is nearly completely transferred to the general base, at a distance of 1.45 Å from the oxygen on C4 and 1.07 Å from the oxygen of the Mg^{2+}-bound hydroxide ion. This results in a more negative partial charge developing on the O4 atom of TS1 compared with the reactant, −0.61 vs −0.44 e, respectively. In addition, the charge on the oxygen atom of the Mg^{2+}-bound HO− is less negative by 0.19 e. A slight increase in the charge on the Mg^{2+} and P atoms between TS1 and the Reactant (+0.03 and +0.06, respectively) also occurs while the charge on the *pro-*R_P oxygen remains unchanged. A hydrogen bond between a Mg^{2+}-bound water molecule (trans to the starting Mg^{2+}-bound HO^- group) and the oxygen of the leaving $-OCH_3$ group develops with a distance of 1.65Å and the P−OCH_3 distance has increased to 1.78 Å. This pattern of hydrogen bonds between the internal nucleophile and the departing $^-OCH_3$ moiety is dictated by the octahedral coordination geometry preferred by Mg^{2+} ions and allows for the specific orientation of the HO^- and H_2O for catalysis. Further, the change in these hydrogen-bonding interactions relative to the reactant structure indicates a considerable strengthening which is maintained in the intermediate structure (vide infra). The negative charge on the departing oxygen has increased to −0.65 e. These results show that this transition state is early with respect to O4−P bond formation yet late with respect to proton transfer.

3.3. The Pentacoordinate Intermediate. A trigonal bipyramidal (TBP) intermediate was distinguished along the reaction coordinate, linking TS1 and TS2 (vide infra). The energy of the intermediate was 18.6 kcal/mol (Table 2) above that of the Reactant, and there were no imaginary frequencies associated with this structure. The intermediate structure is shown in Figure 4 and is characterized by an O4−P distance of 1.98 Å, a P−OCH_3 distance of 1.80 Å, and an O4−P−OCH_3 angle of 157.4° (Table 1). The deviation of the phosphorus from the plane defined by the equatorial oxygen atoms is +4.0°, indicating that inversion of configuration about the phosphorus has not yet occurred. The lengths of the hydrogen bonds of the Mg^{2+}-bound water molecules to the $O4^-$ nucleophile and the oxygen of the OCH_3 leaving group are 1.50 and 1.61 Å, respectively. There were only slight deviations in the charges on the Mg^{2+} ion and phosphate group atoms in the intermediate structure vs TS1 (and TS2), suggesting that little charge transfer occurs between the Mg^{2+} cation and the phosphate of compound **I** (data not shown). The location of a pentacoordinate intermediate is consistent with the observations by Westheimer[13] who found that endocyclic hydrolysis of cyclic phosphate esters proceeds via an intermediate structure that is similar to an S_N2 process. In addition, exocyclic cleavage in the pH range of 4−11[60] has been proposed to occur through an intermediate structure similar to that obtained here. Support for the presence of a TBP intermediate was provided by the determination of a stable pentaoxyphosphorane species via X-ray crystallography.[61]

3.4. The Rate-Determining Step, Transition State 2. The search for a transition state corresponding to departure of the $-OCH_3$ group of compound **I** resulted in the location of a second transition state (TS2) shown in Figure 5. The activation energy (ΔE_{total}) for this structure was calculated to be 20.8 kcal/mol higher in energy than the Reactant (Table 2). The TS2 structure has one imaginary frequency at -395 cm^{-1}, which corresponds to a P−OCH_3 bond-breaking event coupled with a transfer of a proton from Mg^{2+}-bound water, to assist in the departure of the leaving group as methanol. TS2 is also an asymmetric transition state with an O4−P distance of 1.84 Å, a P−OCH_3 bond distance of 1.96 Å, and an O4−P−OCH_3 angle of displacement of 157.8°, slightly larger than in TS1 and the intermediate structure (Table 1). In TS2, the deviation of the

(60) Kluger, R.; Covitz, F.; Dennis, E. A.; Williams, L. D.; Westheimer, F. H. *J. Am. Chem. Soc.* **1969**, *91*, 6066−6072.
(61) Hamilton, W. C.; LaPlaca, S. J.; Ramirez, F. *J. Am. Chem. Soc.* **1965**, *87*, 127−128.

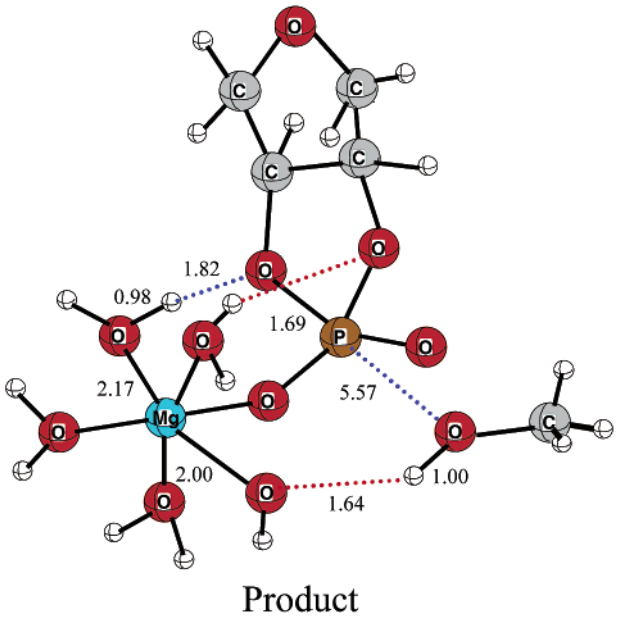

Figure 6. Structure of the optimized product of the hydrolysis reaction.

phosphorus atom from the plane defined by the equatorial oxygen atoms is −3.5°, indicating that inversion of configuration about the phosphorus has taken place. The hydrogen bond between the transferred proton and the internal nucleophile ($O4^-$) has lengthened to 1.76 Å, while the hydrogen bond between the trans Mg^{2+}-bound water molecule and the oxygen of the $-OCH_3$ leaving group has shortened considerably, to 1.28 Å, to assist in its departure. There was no change in the charge on the *pro*-R_P oxygen or phosphorus atoms between TS1 and TS2, while only slight charge changes (maximum +0.02 e) were evident in the remaining phosphate oxygen atoms. Here, O−P bond breaking appears to be late, while the proton transfer is early.

3.5. Hydrolysis Product. Following proton transfer from the trans Mg^{2+}-bound water molecule, regenerating the $Mg^{2+}(HO^-)$ (aq) cofactor, the oxygen of the methanol product has migrated 5.57 Å away from the phosphorus atom (Table 1) of the cyclic phosphate of 3,4-dihydroxydihydrofuran product containing the bound cofactor. The free energy of the hydrolysis products was found to be 2.3 kcal/mol below that of the reactant (Table 2), thus, the overall reaction including solvation and entropy effects is exergonic. Here, the phosphorus atom is below the plane defined by the equatorial oxygen atoms by 23.2°. In addition, hydrogen bonds involving the important functional groups are maintained and shown in Figure 6.

3.6. Reaction Coordinate. The rate-determining step in the divalent metal ion-catalyzed hydrolysis of the hammerhead ribozyme has been determined to be the departure of the 5′O^- leaving group.[11,12,14] The rate-limiting step corresponds to the highest point (TS2) on the potential energy surface in our calculations of compound **I**, as shown in Figure 7. The total accumulated activation energy barrier is 20.8 kcal/mol. The tightening of hydrogen bonds in the transition states suggests that they provide considerable assistance in the catalysis of hydrolysis.[55−58] Examination of the curve suggests that the lifetime of the intermediate structure is very limited, and would appear to be kinetically insignificant[62,63] along the reaction pathway. From TS1 to TS2, substantial changes in geometry occur with only a small change in energy (∼2 kcal/mol). It can

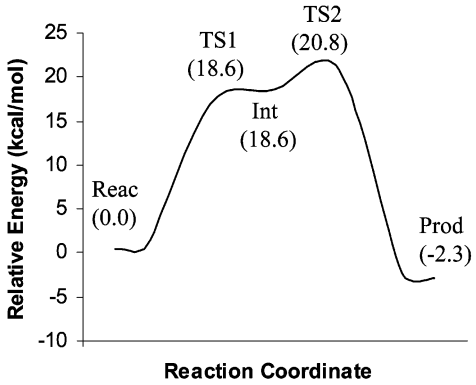

Figure 7. Relative energies, including solvation effects, for the transesterification reaction for the model phosphodiester compound **I**.

be seen that the structure of TS1 corresponds to the transition state for endocyclic cleavage, while the structure of TS2 corresponds to that for exocyclic cleavage. Therefore, this reaction does not appear to proceed by a simple concerted mechanism. Experimental studies on methyl ethylene phosphate have determined that the activation energy for its hydrolysis is ca. 7.5 kcal/mol greater than that for the hydrolysis for trimethyl phosphate.[64] The calculated energy difference, including solvation effects, between the two transition states of **I** (2.1 kcal/mol) is comparable to these experimental findings, although the calculations slightly underestimate this barrier. In addition, the calculated overall energy barrier is consistent with the reported value of the rate-determining step of approximately 1 min^{-1} (∼20 kcal/mol) found in vitro for the autocatalysis reaction involving divalent metal ions for hammerhead ribozyme.[3,8]

4. Conclusions

In the current study, metal-ligated water is involved in creating the nucleophile and assisting the departure of the leaving group, suggested by experimental[9,10,14,15,22−24] and molecular dynamics studies.[36,37] The divalent metal ion serves as a Lewis acid to assist in nucleophilic addition by associating with the *pro*-R_P oxygen of the negatively charged phosphate moiety of the substrate. Our calculations also provide evidence for the additional postulated roles of metal ions in catalysis.[65] These include the following: (1) orienting the ligated water molecules for catalysis and providing hydrogen bonds to stabilize the developing negative charges on the internal nucleophile and the leaving group, (2) providing a hydroxide ion near the scissile phosphate to generate the nucleophile and promote catalysis, and (3) facilitating the loss of leaving group via donation of a proton from a metal-ligated water molecule. Molecular dynamics studies[32−37] have suggested that a pucker in the *S* domain (C2′-*endo* in nucleosides) is necessary for catalysis by the internal nucleophile, which is confirmed by our calculations. It can be seen that in this model nucleophilic displacement is facilitated by a divalent metal ion binding to phosphate and the reaction proceeds with the required proton

(62) Dejaegere, A.; Lim, C.; Karplus, M. *J. Am. Chem. Soc.* **1991**, *113*, 4353−4355.
(63) Taira, K.; Uchimaru, T.; Storer, J. W.; Yliniemela, A.; Uebayasi, M.; Tanabe, K. *J. Org. Chem.* **1993**, *58*, 3009−3017.
(64) Kaiser, E. T.; Panar, M.; Westheimer, F. H. *J. Am. Chem. Soc.* **1963**, *85*, 602−607.
(65) Benkovic, S. J.; Shray, K. J. In *Transition States of Biochemical Processes*; Gandour, R. D., Schowen, R. L., Eds.; Plenum Press: New York, 1978; pp 493−527.

transfers. Little additional electrostatic stabilization is afforded to the reactant compared to the transition states (TS1 and TS2) or the intermediate by the divalent metal ion during the reaction, although it appears that the divalent metal ion mediates the charge changes that occur. In addition, applying solvation, zero-point, and entropy corrections to the gas-phase activation energies results in a lowering of the activation energy barrier to make the reaction accessible. The rate-determining transition state, TS2, located in this study shows that one metal ion is sufficient to catalyze the self-cleavage of the hammerhead ribozyme. Although gas-phase calculations alone are limited in their significance to the reaction in solution, these calculations plus corrections provide structures and final energies consistent with experimental results and indicate that, at the present level of theory, the reaction is stepwise. The possibility of two metal ions participating in the cleavage reaction, however, cannot be eliminated. It is hoped that these results will aid in the development of antisense therapeutics.

Acknowledgment. This work was supported by a grant from the National Institutes of Health to David. A. Case (GM56879). We thank W. W. Cleland for his helpful comments. F.H. would like to thank the Wenner-Gren Foundation for a postdoctoral fellowship.

JA021451H